Ion Speciation and Transport Properties of LiTFSI in 1,3-Dioxolane Solutions: a Case Study for Li–S Battery Applications

Rinaldo Raccichini[*,†], *James W. Dibden*[†], *Ashley Brew*[‡], *John R. Owen*[*,†], *and Nuria García-Aráez*[*,†]

[†]University of Southampton, Department of Chemistry, Southampton, SO17 1BJ, UK

[‡]OXIS Energy Ltd, E1 Culham Science Centre, Abingdon, OX14 3DB, UK.

Corresponding Authors

*R.Raccichini@soton.ac.uk (ORCID ID: 0000-0003-1507-2739); *J.R.Owen@soton.ac.uk (ORCID ID: 0000-0002-4938-3693); *N.Garcia-Araez@soton.ac.uk (ORCID ID: 0000-0001-9095-2379)

ABSTRACT: The Lithium–Sulfur battery is considered to be one of the main candidates for the “post-lithium-ion” battery generation, because of its high theoretical specific capacity and inherently low cost. The role of the electrolyte is particularly important in this system and remarkable battery performances have been reported by tuning the amount of salt in the electrolyte. To further understand the reasons for such improvements we chose the lithium bis(trifluoromethanesulfonyl)imide in 1,3-dioxolane electrolyte as a model salt-solvent system for a systematic study of conductivity and viscosity over a wide range of concentration from 10^{-5} up to 5 molal. The experimental results, discussed and interpreted with reference to the theory of electrolyte conductance, lead to the conclusion that triple ions formation is responsible for the highest molal conductivity values before reaching the maximum at 1.25 molal. At higher concentrations, the molal conductivity drops quickly due to a rapid increase in viscosity and the salt–solvent system can be treated as a diluted form of molten salt.

INTRODUCTION

Lithium–sulfur batteries (LSBs) stand out as one of the most promising and viable candidates for the next generation of rechargeable batteries with higher specific energy than what is possible with lithium-ion battery technology.[1] Indeed, cells with energy densities matching that of Li-ion cells have been recently reported[2,3] and LSBs have been already considered for industrial development.[2] Strategies toward progress of innovative sulfur-containing cathodes,[4] protection of the lithium metal anode,[5] use of functionalized separators,[6,7] as well as the employment of performance-improving electrolytes[1,2,8–13] seem to be very effective. Concerning the electrolyte component, various attempts addressing the conventional drawbacks for LSB electrolytes (e.g., polysulfide dissolution and shuttling issues, and/or low conductivity at high concentration) have been widely reported in the literature.[8,14–19] Particularly, in 2013, Armand et al.[20] demonstrated a new class of liquid "Solvent-in-Salt" electrolytes (analogous to the "Polymer-in-Salt" concept for solid-state-based electrolytes previously developed by Angell[21]) with a weight or volume ratio of salt-to-solvent greater than one, using an ether-based solvent and a fluorinated salt. Enhanced cycling stability, high practical capacity, excellent rate capability, and an almost unitary Coulombic efficiency were reported for the most concentrated electrolyte solution (*i.e.*, 7 moles of salt in 1 L of binary solvent mixture).[20]

The present work aims to further the understanding of the ion speciation and transport properties over a wide range of concentrations. For this study we chose using the largely employed electrolyte solution formed by lithium bis(trifluoromethanesulfonyl)imide (LiTFSI) salt in 1,3-dioxolane (DOL) solvent, at unusually high concentrations up to 5 molal. Crystalline LiTFSI possesses a low dissociation energy, but not the lowest, in the category of Li–containing salts of weakly coordinating anions[22,23] where the Li^+–anion interactions are weakened[15,20] due to charge

delocalisation in the anion. Moreover, the ethereal oxygen atoms of the aprotic Lewis base DOL strongly coordinate Li^+,[24] further aiding dissolution of LiTFSI, and the consequent availability of Li^+ ions. DOL has a low dielectric constant (*i.e.*, ca. 7 at 25 °C)[25] which encourages the formation of neutral ion pairs,[26] decreasing the molal conductivity of all but extremely dilute concentrations.[27] Although we observed this effect quantitatively, our main interest is in the changes in molal conductivity due to the subsequent effects of triple ions formation and large increases in viscosity in the concentrated region (*i.e.*, where molality is greater than 1), where this class of electrolyte starts behaving like a diluted form of a molten salt as suggested by Reddy et al.[28] two decades ago. The Fuoss–Onsager–Hsia–Fernandez–Prini equation,[26,29–31] often used to describe the conductivity in the presence of triple ions, is relatively complex and relies on a number of parameters and assumptions that may not be valid in our study. Therefore, our alternative approach is to divide the concentration range into sections and apply very simple models with a minimum number of parameters analysis for each section.

RESULTS AND DISCUSSION

Figure 1 shows the conductivity (κ) and molal conductivity (Λ_m) for various LiTFSI–DOL electrolyte solutions in the study. As expected, the conductivity increases with the increase of the salt concentration (Figure 1a) up to a maximum value of around 7.44 $mS \cdot cm^{-1}$ at about 2.5 molal (Figure 1a inset, Supporting Information S1 and Table S1.1) but subsequently decreases until saturation at ca. 5 molal. Dividing the conductivity by the molal concentration (c) of the salt, we obtain the molal conductivity Λ_m (Figure 1b), which shows a behaviour similar to that reported for poly(ethylene oxide)-based electrolytes,[27] first decreasing to a minimum value of 0.43 $mS \cdot kg \cdot mole^{-1} \cdot cm^{-1}$ at about 0.04 molal (Table S1.1), then increasing reaching a molal

conductivity maximum of 4.51 mS·kg·mole^{-1}·cm^{-1} at 1.25 molal. A final decrease of the molal conductivity occurs on further increasing the concentration toward the saturation limit.

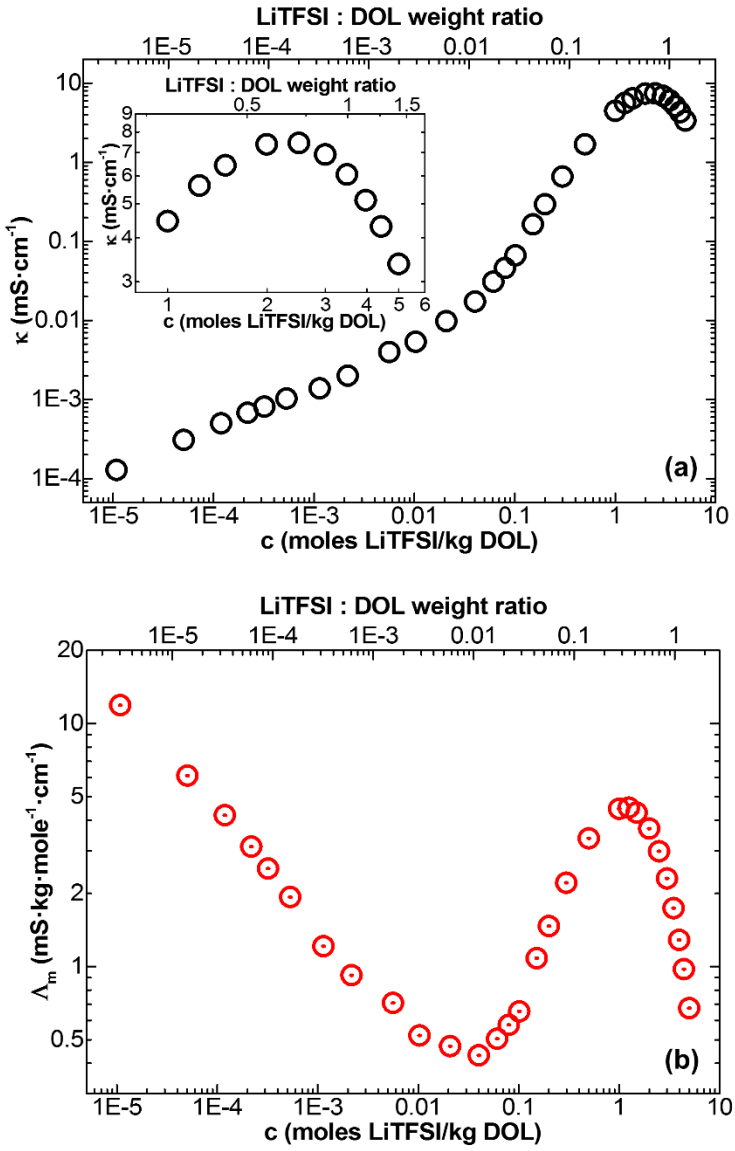

Figure 1. Electrolyte conductivity (a + inset) and molal conductivity (b) as a function of the molal concentration for different LiTFSI–DOL electrolyte solutions at 25°C (all the axis are in logarithmic scale).

The main problems in analysing conductivity behaviour in solutions are to identify the contributions of different ions to the overall conductivity, and to separate the effect of the concentrations of the ions c_i from their mobilities μ_i in the general expression for the conductivity:[32]

$$\kappa = \sum_i z_i F c_i \mu_i = z_+ F c_+ \mu_+ + z_- F c_- \mu_- \quad \text{(for a 1:1 electrolyte)} \quad \text{(Equation 1)}$$

Where subscripts + and – stand for the cation and the anion, z_i is the charge of an ion *i* and, *F* is Faraday's constant. The molal conductivity is defined as:[32]

$$\Lambda_m = \kappa / c \quad \text{(Equation 2)}$$

where c is the nominal molal concentration of the salt.[⊥] Determination of the concentrations of the ionic species, c_+ and c_-, is difficult without additional data, except in the theoretical limit of infinite dilution, at which the salt will fully dissociate and hence $c_+ = c_- = c$. In the limit of infinite dilution, the mobilities of the ions will achieve constant values, and consequently the Λ_m will also become a constant. This value of the molal conductivity is known as limiting molal conductivity, Λ_m^0:

$$\Lambda_m^0 = \sum_i z_i F \mu_i^0 = z_+ F \mu_+^0 + z_- F \mu_-^0 = \lambda_+ + \lambda_- \quad \text{(for a 1:1 electrolyte)} \quad \text{(Equation 3)}$$

where μ_i^0 is the ion mobility of an ion *i* at infinite dilution, λ_i is the limiting molal ionic conductivities of an ion *i* and the subscripts + and – stand for the cation and the anion.

In the case of weak electrolytes, including most solutions of salts in non-aqueous solvents, the variation of conductivity with concentration in the dilute range is predominantly due to association of ions to form neutral solvated ion pairs (Ostwald dilution law). As reported in the literature, Li^+ ions are strongly solvated by ethereal oxygen atoms of the solvent; conversely the $TFSI^-$ anions interact weakly with the solvent molecules and compete with DOL for Li^+ ions

[⊥] The analysis of dilute solutions is usually done using the molar concentration, but for the present case with more concentrated solutions, the use of molal concentration is more accurate.

coordination.[30,33,34] In the case of LiTFSI–DOL salt-solvent system, the following chemical equation can be used to describe the weak electrolyte system:

$$M^+\text{–}(SOL)_4 + X^- \rightleftarrows MX\text{–}(SOL)_3 + SOL \quad \text{(Equation 4)}$$

where M is Lithium, X is the TFSI and SOL is the solvent (*i.e.*, DOL).

For the sake of simplicity the above reaction can be described in terms of simple ions as:

$$Li^+ + TFSI^- \rightleftarrows Li^+\text{–}TFSI^- \quad \text{(Equation 5)}$$

Assuming ideal behaviour, *i.e.*, unit activity coefficients, the equilibrium constant of dissociation of ion pairs into individual ions can be defined as:

$$K_S = [Li^+][TFSI^-]/[Li^+\text{–}TFSI^-] \quad \text{(Equation 6)}$$

The ion concentrations are expressed by the degree of dissociation into simple ions, α_S, and thus $[Li^+] = [TFSI^-] = \alpha_S c$ and $[Li^+\text{–}TFSI^-] = (1 - \alpha_S)c$, where c is the total concentration of the LiTFSI salt. With this, K_s can be expressed as:

$$K_S = \alpha_S^2 c/(1 - \alpha_S) \quad \text{(Equation 7)}$$

which can also be written as:

$$1/\alpha_S = 1 + (\alpha_S c/K_S) \quad \text{(Equation 8)}$$

Assuming that the mobilities of the ions do not change with concentration,[35] the molal conductivity can be expressed as:

$$\Lambda_m = \alpha_S \Lambda_S^0 \quad \text{(Equation 9)}$$

Where Λ_S^0 is the limiting molal conductivity of the salt at infinite dilution (see also Equation 3). Combination of Equations 8 and 9 gives:

$$1/\Lambda_m = 1/\Lambda_S^0 + [\Lambda_m c/K_S(\Lambda_S^0)^2] = 1/\Lambda_S^0 + [\kappa/K_S(\Lambda_S^0)^2] \quad \text{(Equation 10)}$$

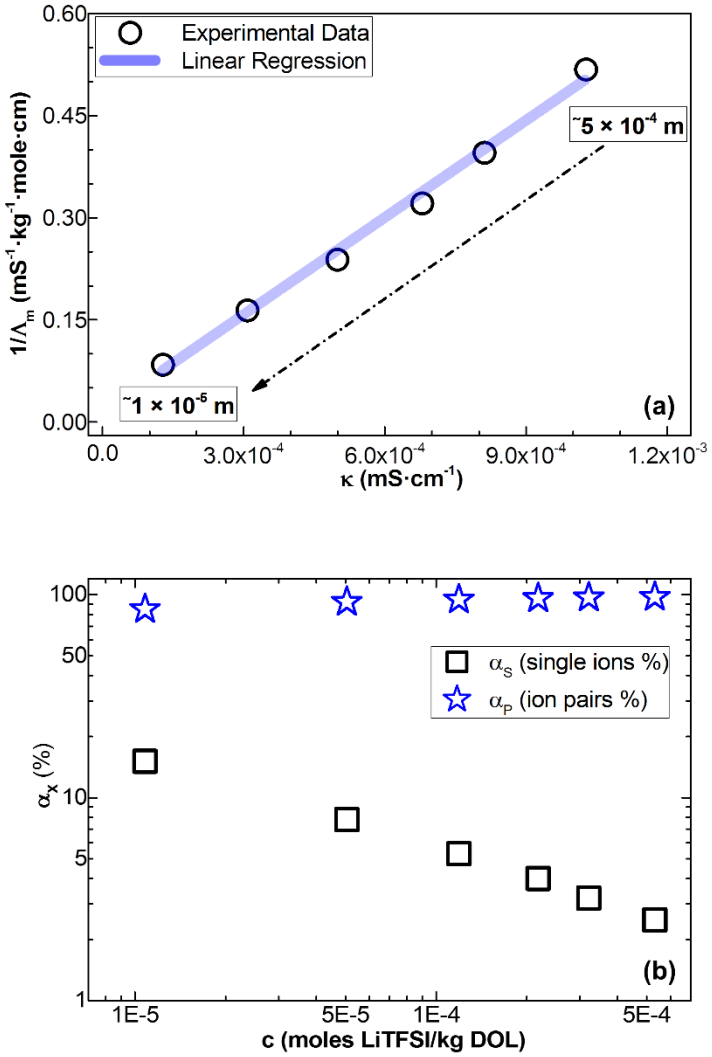

Figure 2. (a) Plot of the reciprocal of the electrolyte molal conductivity vs. the electrolyte conductivity for the most dilute LiTFSI–DOL electrolyte solutions at 25°C (y = 0.01273 + 475.6x ; R^2 = 0.992); (b) Fraction percentage of ion pairs and single ions calculated using the Ostwald dilution law (note that axis are in logarithmic scale).

Equation 10 predicts that the plot of $1/\Lambda_m$ *vs.* κ would give a straight line. This plot (shown in Figure 2a), gives a reasonably constant gradient and intercept in the most dilute region from which Λ_S^0 can be estimated as approximately 80 mS·kg·cm^{-1}·mole^{-1}. The calculated value is in agreement with the estimated Λ_S^0 of ca. 90 mS·kg·cm^{-1}·mole^{-1} obtained using the literature values (see

Supporting Information S2). The amounts of salt present as single ions (α_S) and ion pairs ($\alpha_P = 1-\alpha_S$) according to Equation 9 are shown in Figure 2b (numerical value of the ions fractions are reported in Table S2.1).

For concentrations between 1×10^{-3} molal and 0.1 molal, the experimental data can be described by taking into account the formation of both ion pairs and triple ions as shown in Equation 11 following Fuoss and Kraus.[35] For the LiTFSI–DOL salt–solvent system, we propose the formation of *solvated* triple ions:

$$3[\mathrm{MX}-(\mathrm{SOL})_3] \rightleftarrows \mathrm{M_2X^+}-(\mathrm{SOL})_6 + \mathrm{MX_2^-}-(\mathrm{SOL})_2 + \mathrm{SOL} \qquad \text{(Equation 11)}$$

which may be written as follows for the sake of simplicity:

$$3[\mathrm{Li^+}-\mathrm{TFSI^-}] \rightleftarrows (\mathrm{Li^+})_2-\mathrm{TFSI^-} + \mathrm{Li^+}-(\mathrm{TFSI^-})_2 \qquad \text{(Equation 12)}$$

In this case the simplified Fuoss-Kraus equation[35] (Equation 13a or 13b) describes the molal conductivity as a function of total salt concentration with weak dissociation of ion pairs into single and triple ions (see Supporting Information S3 for the mathematical treatment of the various chemical equations):

$$\Lambda_m = (K_S^{1/2}\Lambda_S^0)c^{-1/2} + (K_S^{1/2}K_T^{-1}\Lambda_T^0)c^{1/2} \qquad \text{(Equation 13a)}$$

or

$$\Lambda_m c^{1/2} = (K_S^{1/2}\Lambda_S^0) + (K_S^{1/2}K_T^{-1}\Lambda_T^0)c \qquad \text{(Equation 13b)}$$

Where K_S and K_T are the dissociation constants of ion pairs to single ions and of triple ion pairs to ion pairs and single ions, respectively.

Λ_S^0 and Λ_T^0 represent the limiting molal conductivities of the single ions and triple ions. Using the value of Λ_S^0 calculated above, a value of Λ_T^0 can be estimated using the approximation:

$$\Lambda_T^0 \approx 2/3\Lambda_S^0 \qquad \text{(Equation 14)}$$

due to Boileau and Hemery,[36] assuming spherical ions with limiting equivalent conductances inversely proportional to the radii.[27,37] Thus we found a value of Λ_T^0 approximately equal to 50 $mS \cdot kg \cdot cm^{-1} \cdot mole^{-1}$. As shown in Figure 3a, a plot of $\Lambda_m c^{1/2}$ *vs.* c is approximately linear as expected from Equation 13b in the concentration range from 1×10^{-3} molal to 0.1 molal. Thus the gradient and intercept can be used to obtain $K_S \approx 2 \times 10^{-7}$ $kg \cdot mole^{-1}$ and $K_T \approx 2 \times 10^{-2}$ $kg \cdot mole^{-1}$. We can also estimate (see Supporting Information S3 for details) the fraction of single ions (*i.e.*, α_S), triple ions (*i.e.*, α_T) and ion pairs (*i.e.*, α_P) as a function of salt concentration as shown in Figure 3b (numerical value of the ions fractions are summarized in Table S3.1).

The simplified Fuoss-Kraus equation is a good approximation to describe the molal conductivity behaviour around the molal conductivity minimum (at 0.04 molal). The form of this equation expressed as Equation 13a shows that there are two contributions to the molal conductivity:

(i) The contribution due to single ions that scales with $c^{-1/2}$. This is the dominant contribution at concentrations below the molar conductivity minimum, and because of that, it is seen that the plot of log Λ_m *vs.* log c has a slope close to -0.5 (Figure 1b, note the logarithmic scale in the plot).

(ii) The contribution due to triple ions that scales with $c^{1/2}$. This term dominates at concentrations higher than the molal conductivity minimum. The plot of log Λ_m *vs.* log c (Figure 1b) has a slope close to 0.5 between the molar conductivity minimum (0.04 molal) and 0.1 molal. This justifies the use of the simplified Fuoss-Kraus equation.

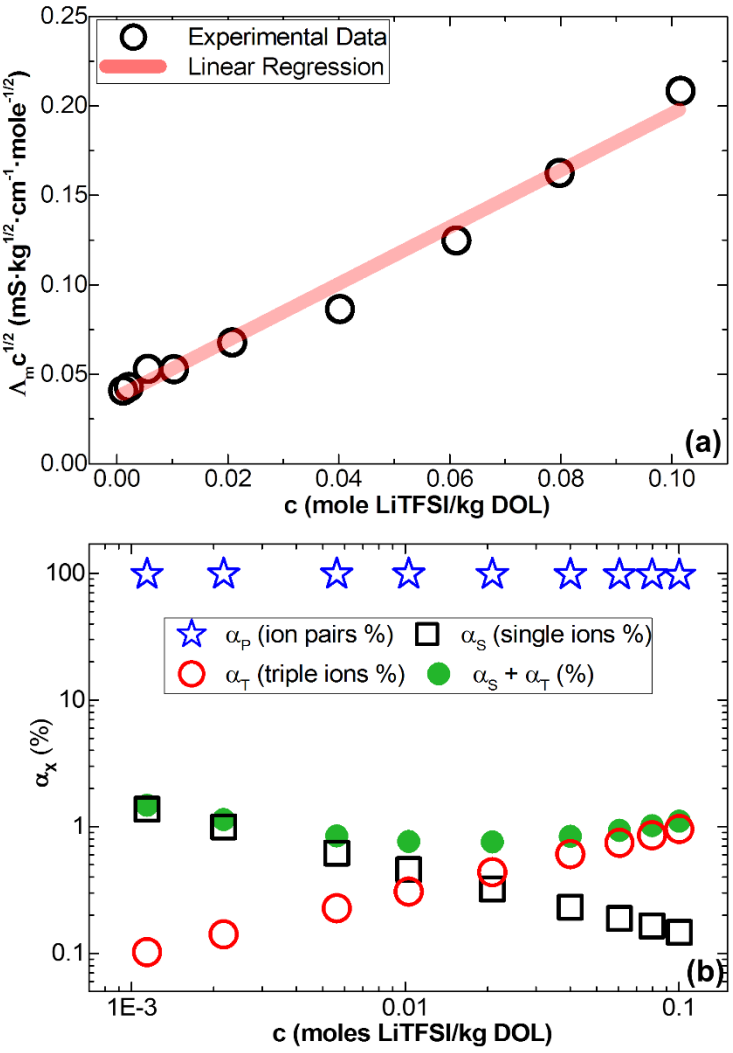

Figure 3. (a) Plot of the electrolyte molal conductivity multiplied by the square-root of the molal concentration *vs*. the molal concentration for various diluted LiTFSI–DOL electrolyte solutions at 25°C ($y = 0.0364 – 1.5863x$; $R^2 = 0.982$); (b) Fraction percentage of single ions, ion pairs and triple ion pairs calculated applying the simplified Fuoss-Kraus relation (note that axis are in logarithmic scale).

However, at concentrations higher than 0.1 molal, which are relevant for LSBs, the simplified Fuoss-Kraus equation fails to describe the experimental data, where it is seen that the log Λ_m *vs.* log c (Figure 1b) has a slope close to 1. Further work is required to explain such an unusually high increase of molal conductivity with concentration in this transition regime region that might be associated with change in ionic mobility and/or activity coefficient of those electrolyte solutions.[38] As observable in Figure 1b, at concentrations higher than 1.25 molal, the molal conductivity starts to decrease. This is related to the rapid increase of the dynamic viscosity η (see Figure 4a and Table S4.1) due to solvent starvation.

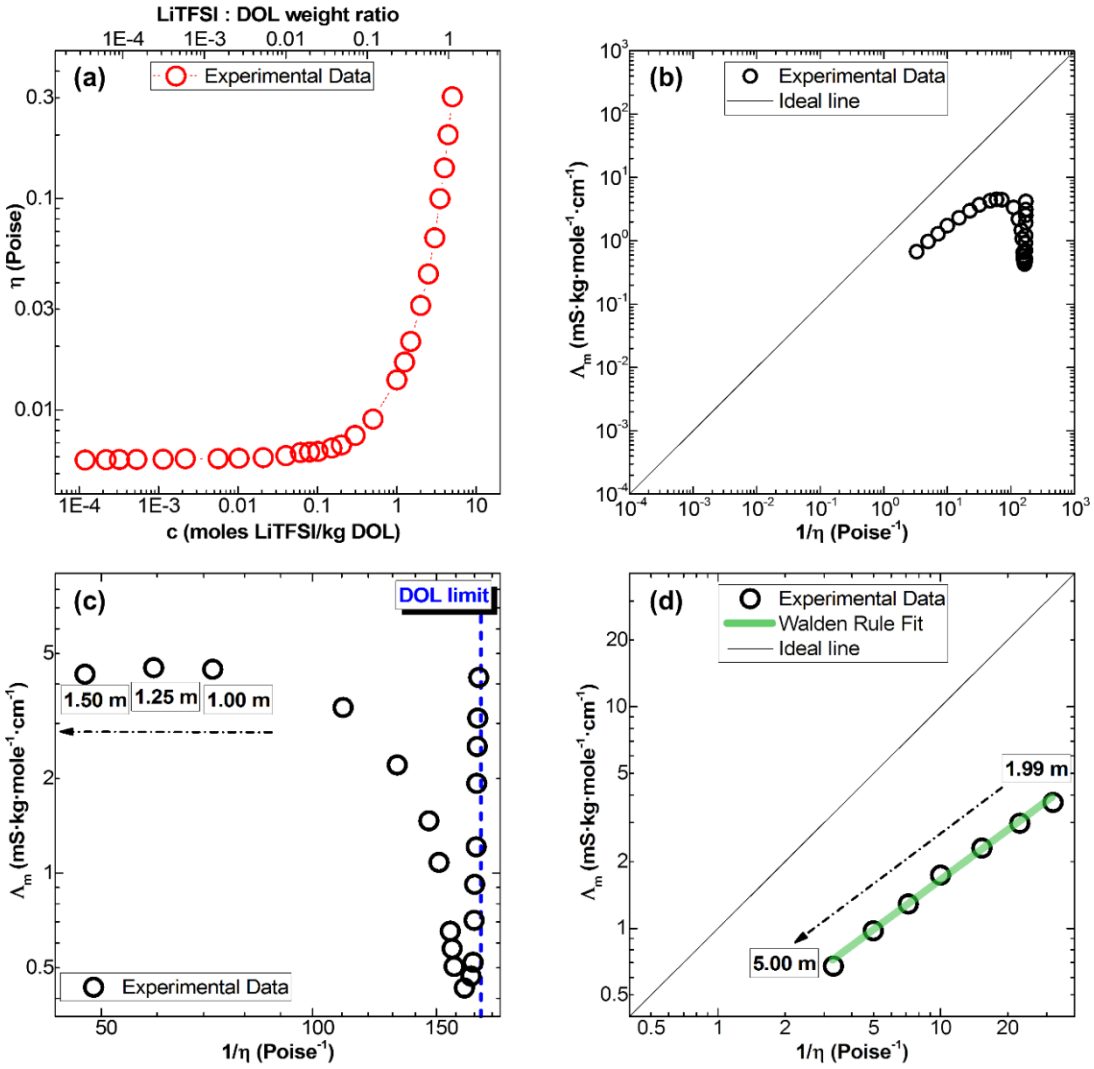

Figure 4. (a) Dynamic viscosity for the various LiTFSI–DOL solutions at 25°C (note that axis are reported in logarithmic scale); (b) Walden plot for all the various LiTFSI–DOL solutions at 25°C (the straight line indicates the ideal behaviour of a line passing through the origin with γ=1, see Equation 15b); (c) Rescaled Walden plot for concentrations up to 1.50 molal (the open circles correspond to the experimental data, the dotted bold blue line represents the fluidity asymptote for the bare solvent DOL); (d) Rescaled Walden plot for concentration ranging from 1.99 molal up to 5.00 molal (the open circles correspond to the experimental data, the green bold straight line represent the fractional Walden rule fit (R^2 = 0.994) and the thin black straight line indicates the ideal behaviour with γ=1).

The LiTFSI/DOL weight ratio increases from approximately 0.36 at a concentration of 1.25 molal to ca. 1.43 at the solubility limit. Therefore, the idea of the ionic atmosphere is hardly appropriate at the highest concentrations.[28] For this reason the highly concentrated solutions are better regarded as a diluted form of a molten salt[28] where a quantitative treatment of the conductivity can be given by the fractional Walden rule:[39]

$$\Lambda_m \eta^\gamma = C \qquad \text{(Equation 15a)}$$

$$\log \Lambda_m = \log C + \gamma \log(1/\eta) \qquad \text{(Equation 15b)}$$

where C is defined as the Walden constant and the exponent γ is ranging from 0 and 1. Generally, the Walden plot (Figures 4b-d) of a specific molten salt[40] is produced by measuring its conductivity and viscosity at different temperatures. However, in this study, the temperature was held at 25 °C and the variable parameter was the salt concentration.

As shown in Figure 4c, going from the lowest concentrations up to ca. 4×10^{-2} molal, the fluidity (defined as 1/η) remains almost constant while a consistent decrease of the molal conductivity can be attributed to the association of single ions into ion pairs as discussed above. Subsequently, the molal conductivity increases rapidly, despite a slight decrease in fluidity. We suggest that this is related, at least in part, to the association of ion pairs into triple ions as the concentration increases, as discussed above. Between 1 molal and 1.5 molal, the molal conductivity remains almost constant, which could be ascribed to the fact that the increase in the degree of association

into triple ions is now counterbalanced by a decrease in fluidity. At concentrations greater than or equal to 2 molal (Figure 4d), a strong coupling between molal conductivity and fluidity is observed by the linearity of the plot of log Λ_m *vs.* log $1/\eta$, following the fractional Walden rule, with an exponent of approximately 0.75.

CONCLUSIONS

Summarising, at concentrations less than 1×10^{-3} molal, the molal conductivity of the LiTFSI–DOL salt-solvent system can be described by the weak electrolyte model (*i.e.*, Ostwald dilution law). For concentrations ranging from 1×10^{-3} to 0.1 molal, Λ_m can be approximately described by the simplified Fuoss-Kraus equation. However, at concentrations higher than 0.1 molal, the observed variation of molal conductivity with concentration is greater than that predicted by the simplified Fuoss-Kraus equation. At concentrations above 1.25 molal, the molal conductivity decreases with concentration because of a marked increase in viscosity, as described by the Walden rule. Figure 5 shows a schematic illustration of the effect of the salt concentration on the ionic species present at various concentrations. Combining the Ostwald dilution law and the simplified Fuoss-Kraus equation, we conclude that for concentrations between 10^{-4} and 0.01 molal, the dissolved LiTFSI salt in DOL is in the form of ion pairs (as the majority species) and single ions. Then, the increase in concentration leads to triple ions formation, and as a result, the molal conductivity increases. When the concentration is higher than around 0.1 molal (*i.e.*, in the transition regime region), the experimental data cannot be described by the simplified Fuoss-Kraus equation. However, we suggest that the number of triple ion pairs will increase at the expense of the number of ion pairs. Finally, at concentrations higher than around 1 molal the LiTFSI-DOL solutions behave as diluted molten salts following the fractional Walden rule. For

this latter region we suggest that LiTFSI salt might be present as triple ions but presumably also in higher extent of ionic association.

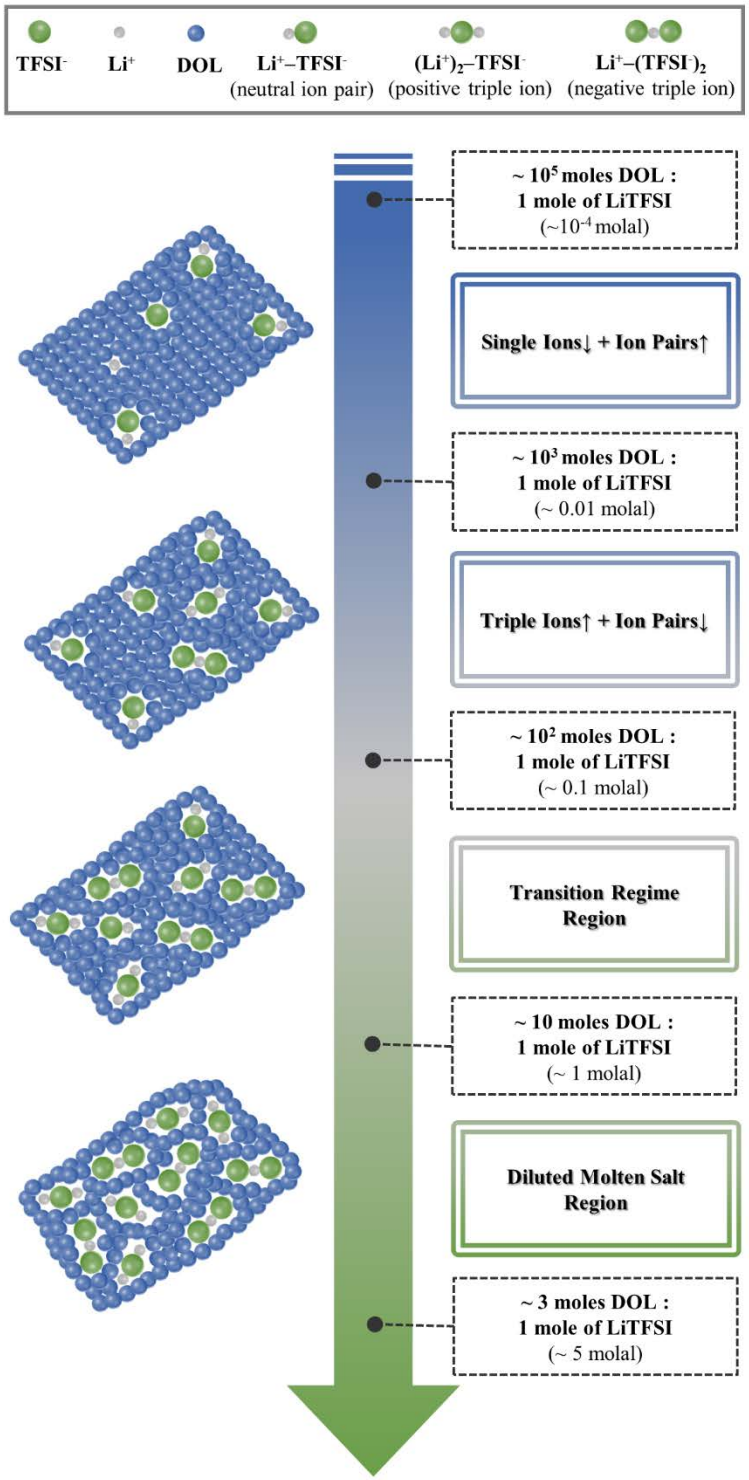

Figure 5. Schematic representation of the effect of the salt concentration on the ionic species present at various concentrations. The symbols ↑ and ↓ indicate the increase and the decrease, respectively, of the various ionic species upon increment of molal concentration.

As a final point, Figure 6 compares our experimental results with the *hypothetical* molal conductivity that would be obtained if the increase in viscosity with concentration could be avoided. The latter is calculated by multiplying the experimental molal conductivity (*i.e.*, Λ_m) by the ratio of viscosity of the various electrolyte solutions divided by the viscosity of the pure solvent (*i.e.*, DOL). It is observed that, by correcting for viscosity factors, the molal conductivity increases proportionally with concentration (*i.e.*, the slope log $\Lambda_m \cdot (\eta_{electrolyte}/\eta_{DOL})$ *vs.* log c is close to 1) from around 0.1 molal to saturation. This means that the electrolyte ionic conductivity, κ, is proportional to the square of the salt concentration. This unusual behaviour that leads to remarkable conductivity enhancement (grey dots in Figure 6) deserves further investigation.

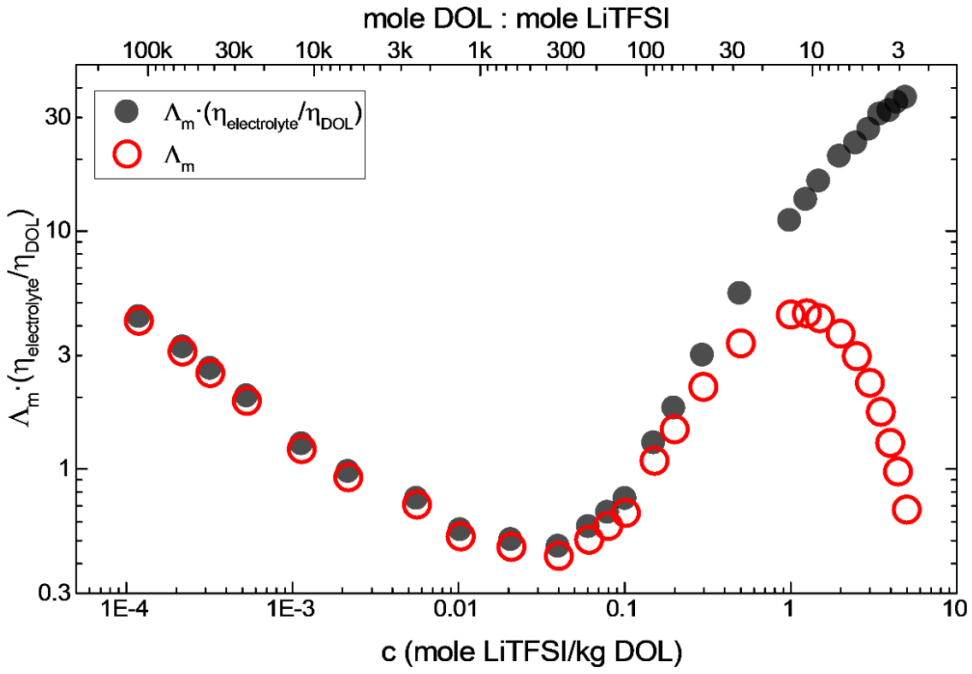

Figure 6. Electrolyte molal ionic conductivity multiplied by the viscosity factor (*i.e.*, $\eta_{electorlyte}/\eta_{DOL}$) as a function of the concentration for different LiTFSI–DOL electrolyte solutions at 25°C (all the axis are in logarithmic scale). Red dots represents the actual electrolyte molal ionic conductivity as also reported in Figure 1b.

In conclusion, we have shown that for the concentrations relevant for applications to LSBs the lithium ions are not significantly present as single ions in solution. Therefore, simplified descriptions of Li-S cell reactions such as:

$$S_8 + 16Li^+ + 16e^- \rightleftarrows 8Li_2S \qquad \text{(Equation 16)}$$

Implicitly neglect the complications associated with changes in the solvation and complexation of lithium ions before they can form the Li_2S precipitate. A systematic study of the effect of solvent on the thermodynamics and kinetics of lithium ions solvation, complexation and conductivity is, therefore, essential in order to understand the effect of solvent in Li-S cell reactions.

ASSOCIATED CONTENT

Supporting Information. The following files are available free of charge.

Experimental methods and data analysis (the latter includes impedance study and conductivity calculations for the various LiTFSI–DOL electrolyte solutions, calculation of the limiting molal conductivity using the Walden rule, derivation of the simplified Fuoss-Kraus equation, calculations of the single ions and triple ions dissociation constants and fractions of solutes, effect of concentration on the viscosity of the various electrolyte solutions).

AUTHOR INFORMATION

Notes

The authors declare no competing financial interests.

ACKNOWLEDGMENTS

This work was supported by OXIS Energy Ltd, the Engineering and Physical Sciences Research Council (EPSRC), Innovate UK, and University of Southampton under the project “Microgrid Energy Storage Using Lithium Sulfur Batteries (MESS)” (EP/P019099/1). J.W.D. acknowledges OXIS Energy Ltd., the University of Southampton and EPSRC (EP/M50662X/1) for a CASE studentship. N.G.A. acknowledges EPSRC (EP/N024303/1) for an early career fellowship. Last but not least, the authors would like to thank Ashley Cooke, Lisset Urrutia, David Ainsworth and Tom Cleaver of OXIS Energy Ltd for the productive scientific discussions.

REFERENCES

(1) Choi, J. W.; Aurbach, D. Promise and Reality of Post-Lithium-Ion Batteries with High Energy Densities. *Nat. Rev. Mater.* **2016**, *1*, 16013.

(2) Manthiram, A.; Chung, S.-H.; Zu, C. Lithium-Sulfur Batteries: Progress and Prospects. *Adv. Mater.* **2015**, *27*, 1980–2006.

(3) Bugga, R. High Energy Density Lithium-Sulfur Batteries for NASA and DoD Applications. In *2nd Lithium Sulfur Batteries: Mechanisms, Modelling and Materials Conference, 25th-26th April 2017, London, UK*.

(4) Zu, C.; Li, L.; Guo, J.; Wang, S.; Fan, D.; Manthiram, A. Understanding the Redox Obstacles in High Sulfur-Loading Li-S Batteries and Design of an Advanced Gel Cathode. *J. Phys. Chem. Lett.* **2016**, *7*, 1392–1399.

(5) Lin, D.; Liu, Y.; Cui, Y. Reviving the Lithium Metal Anode for High-Energy Batteries. *Nat. Nanotechnol.* **2017**, *12*, 194–206.

(6) Conder, J.; Forner-Cuenca, A.; Gubler, E. M.; Gubler, L.; Novak, P.; Trabesinger, S.

Performance-Enhancing Asymmetric Separator for Lithium-Sulfur Batteries. *ACS Appl. Mater. Interfaces* **2016**, *8*, 18822–18831.

(7) Bai, S.; Liu, X.; Zhu, K.; Wu, S.; Zhou, H. Metal–organic Framework-Based Separator for Lithium–sulfur Batteries. *Nat. Energy* **2016**, *1*, 16094.

(8) Pang, Q.; Liang, X.; Kwok, C. Y.; Nazar, L. F. Advances in Lithium–sulfur Batteries Based on Multifunctional Cathodes and Electrolytes. *Nat. Energy* **2016**, *1*, 16132.

(9) Manthiram, A.; Fu, Y.; Chung, S.; Zu, C.; Su, Y. Rechargeable Lithium−Sulfur Batteries. *Chem. Rev.* **2014**, *114*, 11751–11787.

(10) Judez, X.; Zhang, H.; Li, C.; González-Marcos, J. A.; Zhou, Z.; Armand, M.; Rodriguez-Martinez, L. M. Lithium Bis(fluorosulfonyl)imide/Poly(ethylene Oxide) Polymer Electrolyte for All Solid-State Li–S Cell. *J. Phys. Chem. Lett.* **2017**, *8*, 1956–1960.

(11) Zu, C.; Klein, M.; Manthiram, A. Activated Li2S as a High-Performance Cathode for Rechargeable Lithium–Sulfur Batteries. *J. Phys. Chem. Lett.* **2014**, *5*, 3986–3991.

(12) Cuisinier, M.; Cabelguen, P.-E.; Adams, B. D.; Garsuch, A.; Balasubramanian, M.; Nazar, L. F. Unique Behaviour of Nonsolvents for Polysulphides in Lithium-Sulphur Batteries. *Energy Environ. Sci.* **2014**, *7*, 2697–2705.

(13) Cuisinier, M.; Hart, C.; Balasubramanian, M.; Garsuch, A.; Nazar, L. F. Radical or Not Radical: Revisiting Lithium-Sulfur Electrochemistry in Nonaqueous Electrolytes. *Adv. Energy Mater.* **2015**, *5*, 1401801.

(14) Zhang, S.; Ueno, K.; Dokko, K.; Watanabe, M. Recent Advances in Electrolytes for Lithium-Sulfur Batteries. *Adv. Energy Mater.* **2015**, *5*, 1500117.

(15) Younesi, R.; Veith, G. M.; Johansson, P.; Edstrom, K.; Vegge, T. Lithium Salts for Advanced Lithium Batteries: Li-Metal, Li-O2, and Li-S. *Energy Environ. Sci.* **2015**, *8*, 1905–1922.

(16) Al-Mahmoud, S. M.; Dibden, J. W.; Owen, J. R.; Denuault, G.; Garcia-Araez, N. A Simple,

Experiment-Based Model of the Initial Self-Discharge of Lithium-Sulphur Batteries. *J. Power Sources* **2016**, *306*, 323–328.

(17) Dibden, J. W.; Smith, J. W.; Zhou, N.; Garcia-Araez, N.; Owen, J. R. Predicting the Composition and Formation of Solid Products in Lithium-Sulfur Batteries by Using an Experimental Phase Diagram. *Chem. Commun.* **2016**, *52*, 12885–12888.

(18) See, K. A.; Wu, H. L.; Lau, K. C.; Shin, M.; Cheng, L.; Balasubramanian, M.; Gallagher, K. G.; Curtiss, L. A.; Gewirth, A. A. Effect of Hydrofluoroether Cosolvent Addition on Li Solvation in Acetonitrile-Based Solvate Electrolytes and Its Influence on S Reduction in a Li-S Battery. *ACS Appl. Mater. Interfaces* **2016**, *8*, 34360–34371.

(19) Lee, C. W.; Pang, Q.; Ha, S.; Cheng, L.; Han, S. D.; Zavadil, K. R.; Gallagher, K. G.; Nazar, L. F.; Balasubramanian, M. Directing the Lithium-Sulfur Reaction Pathway via Sparingly Solvating Electrolytes for High Energy Density Batteries. *ACS Cent. Sci.* **2017**, *3*, 605–613.

(20) Suo, L.; Hu, Y.-S.; Li, H.; Armand, M.; Chen, L. A New Class of Solvent-in-Salt Electrolyte for High-Energy Rechargeable Metallic Lithium Batteries. *Nat. Commun.* **2013**, *4*, 1481.

(21) Angell, C. A.; Liu, C.; Sanchez, E. Rubbery Solid Electrolytes with Dominant Cationic Transport and High Ambient Conductivity. *Nature* **1993**, *362*, 137–139.

(22) Armand, M. B.; el Moursili, F. E. K. C. BIS PERHALOGENOACY L -OR SULFONYL-IMIDES OF ALKALI METALS, THEIR SOLID SOLUTIONS WITH PLASTIC MATERIALS AND THEIR USE TO THE CONSTITUTION OF CONDUCTOR ELEMENTS FOR ELECTROCHEMICAL GENERATORS. 4,505,997, 1985.

(23) Han, H. B.; Zhou, S. S.; Zhang, D. J.; Feng, S. W.; Li, L. F.; Liu, K.; Feng, W. F.; Nie, J.; Li, H.; Huang, X. J.; et al. Lithium Bis(fluorosulfonyl)imide (LiFSI) as Conducting Salt for Nonaqueous Liquid Electrolytes for Lithium-Ion Batteries: Physicochemical and Electrochemical Properties. *J. Power Sources* **2011**, *196*, 3623–3632.

(24) Olsher, U.; Izatt, R. M.; Bradshaw, J. S.; Dalley, N. K. Coordination Chemistry of Lithium Ion: A Crystal and Molecular Structure Review. *Chem. Rev.* **1991**, *91*, 137–164.

(25) Venkateswaran, A.; Easterfield, J. R.; Davidson, D. W. A Clathrate Hydrate of 1,3-Dioxolane. *Can. J. Chem.* **1967**, *45*, 884–886.

(26) Fuoss, R. M. Review of the Theory of Electrolytic Conductance. *J. Solution Chem.* **1978**, *7*, 771–782.

(27) MacCallum, J. R.; Tomlin, A. S.; Vincent, C. A. An Investigation of the Conducting Species in Polymer Electrolytes. *Eur. Polym. J.* **1986**, *22*, 787–791.

(28) Bochris, J. O.; Reddy, A. K. N. *Volume 1: Modern Electrochemistry*, Second Ed.; Springer US, 1998.

(29) Corti, H.; Crovetto, R.; Fernández-Prini, R. Mobilities and Ion-Pairing in LiB(OH)4 and NaB(OH)4 Aqueous Solutions. A Conductivity Study. *J. Solution Chem.* **1980**, *9*, 617–625.

(30) Seo, D. M.; Borodin, O.; Balogh, D.; O'Connell, M.; Ly, Q.; Han, S.-D.; Passerini, S.; Henderson, W. A. Electrolyte Solvation and Ionic Association III. Acetonitrile-Lithium Salt Mixtures–Transport Properties. *J. Electrochem. Soc.* **2013**, *160*, A1061–A1070.

(31) Mozhzhukhina, N.; Longinotti, M. P.; Corti, H. R.; Calvo, E. J. A Conductivity Study of Preferential Solvation of Lithium Ion in Acetonitrile-Dimethyl Sulfoxide Mixtures. *Electrochim. Acta* **2015**, *154*, 456–461.

(32) Smedley, S. I. *The Interpretation of Ionic Conductivity in Liquids*; Plenum Press: New York, 1980.

(33) Petrowsky, M.; Frech, R.; Suarez, S. N.; Jayakody, J. R. P.; Greenbaum, S. Investigation of Fundamental Transport Properties and Thermodynamics in Diglyme-Salt Solutions. *J. Phys. Chem. B* **2006**, *110*, 23012–23021.

(34) Zhang, C.; Yamazaki, A.; Murai, J.; Park, J. W.; Mandai, T.; Ueno, K.; Dokko, K.; Watanabe, M. Chelate Effects in Glyme/lithium Bis(trifluoromethanesulfonyl)amide Solvate Ionic Liquids, Part 2: Importance of Solvate-Structure Stability for Electrolytes of Lithium Batteries. *J. Phys. Chem. C* **2014**, *118*, 17362–17373.

(35) Fuoss, R. M.; Kraus, C. A. Properties of Electrolytic Solutions. IV. The Conductance Minimum and the Formation of Triple Ions Due to the Action of Coulomb Forces. *J. Am. Chem. Soc.* **1933**, *55*, 2387–2399.

(36) Boileau, S.; Hemery, P. Conductance of Some Tetraphenylboron and Fluorenyl Salts in Tetrahydropyran. *Electrochim. Acta* **1976**, *21*, 647–655.

(37) Salomon, M.; Uchiyama, M. C. Treatment of Triple Ion Formation. *J. Solution Chem.* **1987**, *16*, 21–30.

(38) Safari, M.; Kwok, C. Y.; Nazar, L. F. Transport Properties of Polysulfide Species in Lithium-Sulfur Battery Electrolytes: Coupling of Experiment and Theory. *ACS Cent. Sci.* **2016**, *2*, 560–568.

(39) Angell, C. A.; Ansari, Y.; Zhao, Z. Ionic Liquids: Past, Present and Future. *Faraday Discuss.* **2012**, *154*, 9–27.

(40) Hayes, R.; Warr, G. G.; Atkin, R. Structure and Nanostructure in Ionic Liquids. *Chem. Rev.* **2015**, *115*, 6357–6426.

TOC Graphic

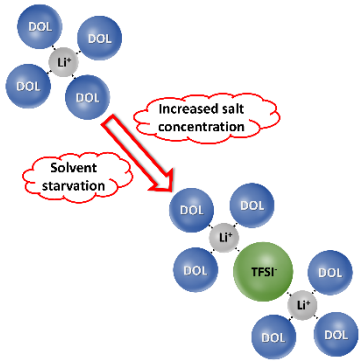
DOL
DOL
Li+
DOL
DOL
Increased salt concentration
Solvent starvation
DOL
DOL
Li+
DOL
TFSI-
DOL
Li+
DOL
DOL